

## Review

UDC 617.3:57.089.67:539.3:539.4

### LONG TERM EVOLUTION OF BONE RECONSTRUCTION WITH BONE GRAFT SUBSTITUTES

*Martynenko O. V.<sup>1</sup>, Zolochovsky O. O.<sup>2</sup>, Allena R.<sup>3</sup>*

<sup>1</sup> V. N. Karazin Kharkiv National University, Kharkiv, Ukraine

<sup>2</sup> National Technical University «Kharkiv Polytechnic Institute», Kharkiv, Ukraine

<sup>3</sup> Arts et Métiers ParisTech, Paris, France

The review involves clinical and experimental data, constitutive modeling, and computational investigations towards an understanding on how mechanical cyclic loads for long periods of time affect damage evolution in a reconstructed bone, as well as, lifetime reduction of bone graft substitutes after advanced core decompression. The outcome of the integrated model discussed in this paper will be how damage growth in femur after advanced core decompression subjected to mechanical cyclic loading under creep and fatigue conditions may be controlled in order to optimize design and processing of bone graft substitutes, and extend lifetime of bone substitutes.

**KEY WORDS:** advanced core decompression, bone graft substitute, damage, stress, creep, fatigue

### ДОВГОСТРОКОВА ЕВОЛЮЦІЯ РЕКОНСТРУКЦІЇ КІСТОК ЗА ДОПОМОГОЮ КІСТКОВИХ ЗАМІННИКІВ – ІМПЛАНТАНТІВ

*Мартиненко О. В.<sup>1</sup>, Золочевський О. О.<sup>2</sup>, Аллена Р.<sup>3</sup>*

<sup>1</sup> Харківський національний університет імені В. Н. Каразіна, м. Харків, Україна

<sup>2</sup> Національний технічний університет «Харківський політехнічний інститут», м. Харків, Україна

<sup>3</sup> Паризький інститут наук та технологій, м. Париж, Франція

Даний огляд включає клінічні та експериментальні дані, визначальні співвідношення, та обчислювальні дослідження, спрямовані на розуміння того як механічні циклічні навантаження протягом тривалих періодів часу впливають на зростання пошкоджуваності і скорочення довговічності імплантатів, що використовуються для компресійного заміщення дефекту кістки. У результаті моделювання, розглянутого в цій статті, буде встановлено як зростання пошкоджуваності протягом механічних циклічних навантажень в умовах повзучості та втоми імплантатів після компресійного заміщення дефекту стегнової кістки можна контролювати з метою оптимізації проектування та виготовлення кісткових заміників- імплантатів і збільшення терміну служби кісткових заміників.

**КЛЮЧОВІ СЛОВА:** компресійне заміщення дефекту кістки, кістковий заміник- імплантат, пошкоджуваність, напруга, повзучість, втома

### ДОЛГОСРОЧНАЯ ЭВОЛЮЦИЯ РЕКОНСТРУКЦИИ КОСТЕЙ С ПОМОЩЬЮ КОСТНЫХ ЗАМЕНИТЕЛЕЙ – ИМПЛАНТАНТОВ

*Мартыненко А. В.<sup>1</sup>, Золочевский А. А.<sup>2</sup>, Аллена Р.<sup>3</sup>*

<sup>1</sup> Харьковский национальный университет имени В. Н. Каразина, г. Харьков, Украина

<sup>2</sup> Национальный технический университет «Харьковский политехнический институт», г. Харьков, Украина

<sup>3</sup> Парижский институт наук и технологий, г. Париж, Франция

Данный обзор включает клинические и экспериментальные данные, определяющие соотношения, и вычислительные исследования, направленные на понимание того как механические циклические нагрузки в течение длительных периодов времени влияют на рост повреждаемости и сокращение

долговечности имплантатов, используемых для компрессионного замещения дефекта кости. В результате моделирования, рассматриваемого в этой статье, будет установлено как рост повреждаемости вследствие механических циклических нагрузок в условиях ползучести и усталости имплантатов после компрессионного замещения дефекта бедренной кости можно контролировать с целью оптимизации проектирования и изготовления костных заменителей - имплантатов и увеличения срока службы костных заменителей.

**КЛЮЧЕВЫЕ СЛОВА:** компрессионное замещение дефекта кости, костный заменитель-имплантат, повреждаемость, напряжение, ползучесть, усталость

## INTRODUCTION

Every year, over two million people worldwide sustain a bone grafting procedure to repair bone defects stemming from a disease or a traumatic event [1].

Core decompression represents an established technique for treatment of early stage osteonecrosis and most commonly used for disease that affects the hip joint. The procedure is designed to decrease pressure within the bone by restoring blood flow to the bone. For the first time, this procedure was popularized by Ficat and Arlet [2] in France in 1980. At present, this technique is one of the most commonly used surgical treatment options.

Core decompression consists of drilling one or more small channels with an 8–10 mm diameter into the necrotic lesion (dead bone) from the lateral subtrochanteric region of femur

to remove an 8–10 mm core from the femoral head [3]. This is associated with a lack of structural support of the bone. Subtrochanteric stress fractures at the surgical entrance point of the core track were regularly described as a complication of conventional core decompression with a rate of about 1–2 % or even higher fracture rate [4]. That is why patients normally are requested to be partial weight bearing for several, normally six weeks due to the risk of fracture.

The so-called advanced core decompression is a modified technique of core decompression that may allow better removal of the necrotic tissue by using a new percutaneous expandable reamer, and refilling of the drill hole and the defect with the implantation of a bone graft substitute (Fig. 1) [3–4]. Such technique gives the possibility to reduce the risk of fracture after surgery.



**Fig. 1.** A proximal femur with the drilling canal and the bone defect filled by a bone graft substitute [4]

Practical recommendations related to the advanced core decompression are mainly based on clinical experience. So there is a need for rigorous studies to determine specific indications for this kind of treatment.

The finite element method has recently become a powerful technique for numerical simulation in the mechanics of femur. A three-dimensional finite element model derived from the reconstruction of core decompression or magnetic resonance (tomographic) images may help to effectively simulate the influences of core decompression on the mechanical behavior of femur.

The finite element studies concerning the advanced core decompression are given in [4]. The impact of the core decompression procedure and the surgical entrance point position on the stress distribution as well as on the fracture risk of the femur has been investigated. The effect of bone substitute stiffness on the biomechanical behavior of femoral bone after core decompression has been studied. Numerical results led to the conclusion that the success of advanced core decompression depends on the amount of necrotic tissue remaining in the femoral head after the procedure. Thus, modifications to the instrument are necessary to increase the amount of necrotic tissue that can be removed. Note also that all these studies are based on the linear elastic behavior of the femur and bone graft substitutes.

Different bone graft substitutes concerning the advanced core decompression have been used, such as a composite calcium sulphate ( $\text{CaSO}_4$ ) – calcium phosphate ( $\text{CaPO}_4$ ), tantalum or low-stiffness implants. The efficiency of these materials is still debated. One of alternative treatments is to use bioresorbable bone graft substitutes [1]. In this regard, the gradient elasticity theory was applied to study the effect of microstructure on remodeling of bones reconstructed with bioresorbable materials. In this way, one – [5], two – [1] and three – dimensional [6] biomechanical models of reconstructed bones have been considered.

Although the short term performance of femur after advanced core decompression is impressive, the long term performance is still unknown. Systematical studies related to the analyze the long term success and the long term risk of failure of bone graft substitute inside a

femoral head after advanced core decompression have not been published so far.

The understanding of bone behaviors and functioning is a key in the ability to predict their evolutions and be able to make adequate diagnostics, surgeries and planning, and predict postoperation states [6].

Biomechanical degradation of femur after advanced core decompression can be related to the load and time dependent phenomena, such as damage, creep and fatigue. These phenomena in bone can be investigated experimentally.

## **OBJECTIVE**

The specific objectives are: to specify the mechanisms of biomechanical degradation of femur after advanced core decompression subjected to mechanical cyclic loading; to develop the constitutive laws of biomechanical behavior and kinetic equations of damage (stiffness reduction, creep, fatigue) in femur after advanced core decompression considering the interaction between osteoblasts and osteoclasts combined with the mechanical response of bone, and taking into account nonlinear elastic deformation and creep under mechanical cyclic loading conditions, fatigue and ratcheting, receiving and healing damage, damage interactions between tension and compression; to identify biomechanical parameters in the proposed bone remodeling model using different experimental data for bone, bone graft substitutes and femur after advanced core decompression; to incorporate an integrated biomechanical constitutive model developed in this research into the ANSYS codes in a form of the computer-based structural modeling tool for analyzing bone density distributions over time, as well as, stress distributions over time in femur after advanced core decompression, for damage analysis and for lifetime predictions of bone graft substitutes; to calculate the time-dependent bone density distribution and time-dependent multiaxial stress distribution (finite element modeling, cell population dynamics, structural mechanics), and changes in damage at a discrete site of bone remodeling (continuum damage mechanics) in femur after advanced core decompression subjected to mechanical cyclic loading as a function of femur parameters, bone graft parameters, as well as, loading conditions, and additionally to predict the lifetime of bone graft substitutes; to find the relationship between bone cell architecture,

bone graft substitute, biological environment, loading conditions and degradation of femur over time after advanced core decompression (combination of 2, 3, 4 and 5); to compare the lifetime predictions obtained in this research against clinical and experimental data available for femur after core decompression in combination with bone substitutes.

**MATERIALS AND METHODS**

**Bone damage.** Mechanically, bone behaves identically to any other material in that it undergoes deformation and damage when subject to an external load. Bone sustains millions of loading cycles over the course of a

lifetime and rarely breaks without a major traumatic event, and, thus, damage in bone is a naturally occurring event [7]. Damage is not detectable using clinical imaging modalities, but decreases bone's stiffness, strength, and toughness and eventually leads to collapse of whole bones [8].

There are three distinct varieties of damage in bone (Table 1), which can be identified as linear microcracks, diffuse microdamage, and microfractures. These types are distinguished by the way they form and their morphology; the nature of the stimuli that cause them to form, as well as, their location; and the manner in which they are repaired [7].

**Table 1**

**Types of damage and their characteristics [7]**

	Shape/ Dimensions	Stress mode	Tissue properties	Predominant location	Age	Repair
Linear Microcracks	Elliptical ~80 x 1 x300 μm	Compressive	More brittle	Interstitial	Older	Remodeling
Diffuse Microdamage	=<10 μm wide Unknown length	Tensile	More ductile	Within trabecular packets and osteons	Younger	Remodeling <sup>1</sup>
Microfractures	Complete fracture	Bending/shear	Off-axis orientation	Trabecular	Older	Endochondral ossification

Obviously that diffuse microdamage means microcracks on a lower length scale. Microcracks appear linear and spatially organized in 2D histological sections with a pertinent length of 10–70 μm [8]. In 3D, microcracks appear in approximately elliptical shape with an aspect ratio of 4:1 to 5:1. In histology studies, tensile microdamage appears to be more diffuse while compressive damage is rather expressed as linear microcrack. Thus, different damage development in tension and compression is a characteristic feature of bone.

Microfractures, on the other hand, are entirely different than the other forms of damage. Microfractures occur within cancellous bone and represent complete fractures of one or more trabeculae [7].

Also, damage interactions between tension and compression in bone have been considered [8-11]. The mechanisms how bone damage is accumulated under different loading modes and coupled into another loading mode have been discussed. Impact of damage interactions on bone strength has been analyzed.

Damage reduces the bone's future capacity to absorb energy prior to fracture, and in this sense deteriorates the mechanical properties of

bone. However, the paradox of this is that the initiation and growth of microcracks in itself dissipates energy and delays a catastrophic complete fracture from occurring [7]. This presumes that the damage will be repaired in an efficient manner, before significantly more damage can be created [12]. This requires a signaling mechanism, and suggests a physiological role, not just a mechanical one, for bone damage [7, 13].

**Creep.** The consideration of the linear elastic deformation of femur after advanced core decompression is quite important in the structural analysis. However, this is not enough in order to understand the mechanisms of degradation of femur over time that affect essentially the lifetime reduction of bone graft substitute inside a femoral head.

It is known [14] that bones exhibit creep deformation considered as a time dependent irreversible deformation process. Both the tensile and compressive creep behaviors of cortical bone and trabecular bone are well documented [15–19]. They are characterized by creep strain versus time curves that have three distinct regimes (Fig. 2) (primary, secondary and tertiary) by analogy with the engineering

materials (steels, cast irons, light alloys) at high temperatures.

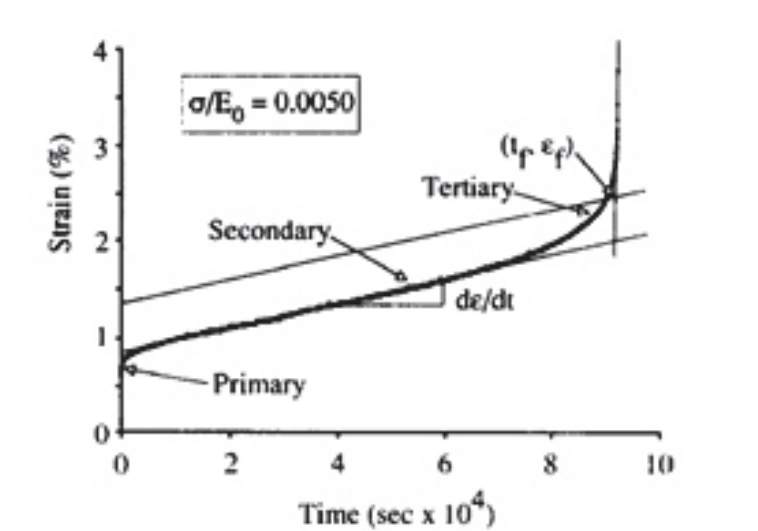


Fig. 2. Typical creep curve for trabecular bone with a time to failure of 25.5 h and a failure strain of 2.5 % [15]

Creep deformation changes the microstructure of bone by introducing microcracks (creep damage) in the final stage of the creep process. Furthermore, the velocity of the growth of already existing microcracks and of the nucleation of new ones essentially depends on the intensity of creep deformation. On the other hand, creep deformation of bone is influenced by the growth of microcracks. This influence begins at the primary and secondary stages of the creep process, and can be visible in the tertiary stage due to increase of the creep strain rate, preceding the creep rupture. The

creep rupture case without increase in the creep strain rate can also be observed in bone. Thus, creep deformation and growth of creep damage in bone occur parallel to each other, and they have a reciprocal effect.

Figure 3 shows stress versus time to failure data in bone for tensile and compressive loading types under creep conditions. All specimens are normalized with Young's modulus. The experimental data are linear on a log-log plot which is similar to power law known for other materials.

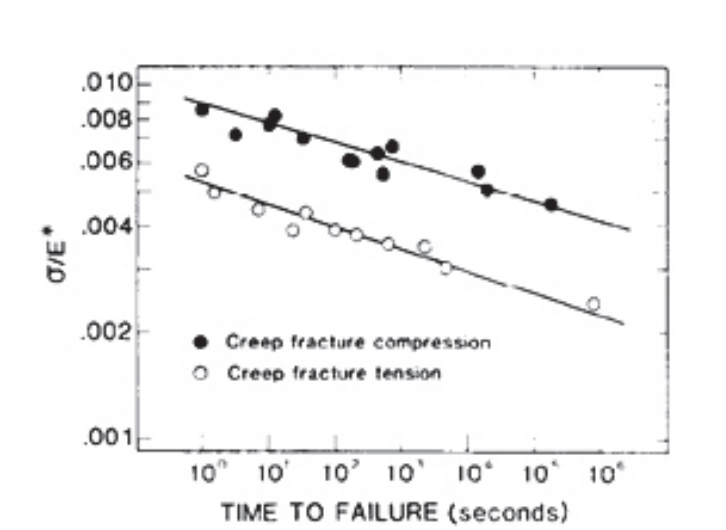


Fig. 3. Experimental creep ruptures data on human femoral cortical bone [20]

Now, a number of comments need to be made. First, creep curves obtained in bone from uniaxial tests under tensile and compressive loading types for one and the same absolute value of constant stress are essentially different and depend on the sign of the stress. This difference can be very large in the tertiary creep state due to the different creep damage growth in tension and compression. Thus, it is necessary to take into account the tension/compression creep asymmetry of femur after advanced core decompression subjected to mechanical cyclic loading. Second, the creep and creep damage parameters of femur in the constitutive model should be a function of the bone density. Third, creep of composite calcium

sulphate ( $\text{CaSO}_4$ ) – calcium phosphate ( $\text{CaPO}_4$ ) has been studied in [21].

**Fatigue and ratcheting.** Among various loading, cyclic loading (including axial, torsional and multiaxial load) plays an important role to damage bone [22]. Damage accumulation under cyclic loading is a major factor of failure in implants.

Fatigue data are extensively reported [22–25] for trabecular part and cortical part of bone. Also, it is found [26] the stiffness loss related to the damage growth in bone (Fig. 4) under cyclic loading. It is seen that stiffness loss under fatigue conditions is dependent on the type of loading.

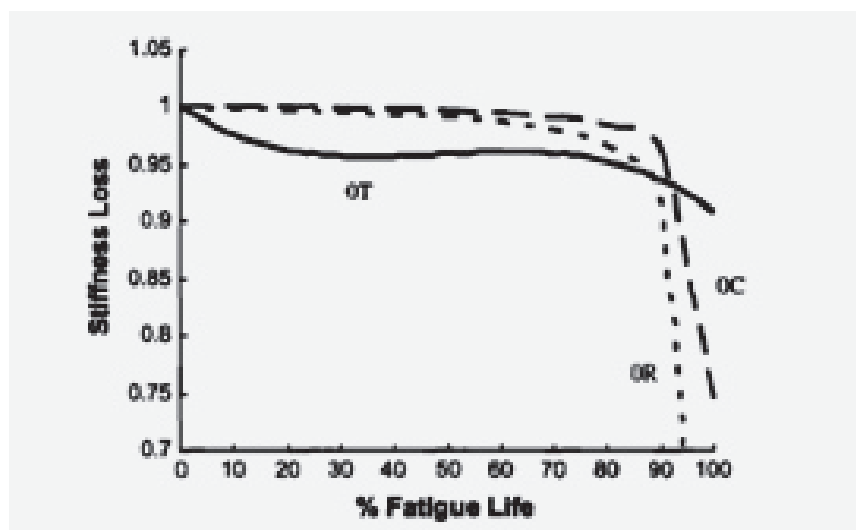


**Fig. 4. Average stiffness loss profiles for specimens subjected to Zero-Tension (0T), Zero-Compression (0C) and zero-Torsion (0T) loading [26]**

Fatigue damage in bone was identified as diffuse damage and linear microcracks using histological analysis [26]. Mode I fracture creates and propagates microcracks in the transverse direction for specimens subjected to Zero-Tension loading (Fig. 5). In contrast, the compressive group displayed Mode II cracking when crack surfaces slide over one another; damage is on a single plane (Fig. 5). Thus, there are differences in the kind of damage associated with fatigue in tension and compression.

Mode III fracture (Fig. 5) for specimens subjected to Zero-Torsion loading is similar to a tearing motion where the crack surfaces move relative to each other on multiple planes .

The fatigue life data for human femoral cortical bone [20] are presented in Fig. 6.

Fatigue tests in specimens subjected to Zero-Tension and Zero-Compression loading were conducted at the two load frequencies (2 and 0.02 Hz). It is seen (Fig. 6) that fatigue lives of bone are longer in compression than in tension.

A comparison of the fatigue behavior of human trabecular and cortical bone tissue [24] was conducted under cyclic four-point bending (Fig. 7). The results show that trabecular specimens have significantly lower fatigue strength than cortical specimens, despite their higher mineral density values. Thus, the parameters of femur in the kinetic equation of fatigue damage should be a function of the bone density.

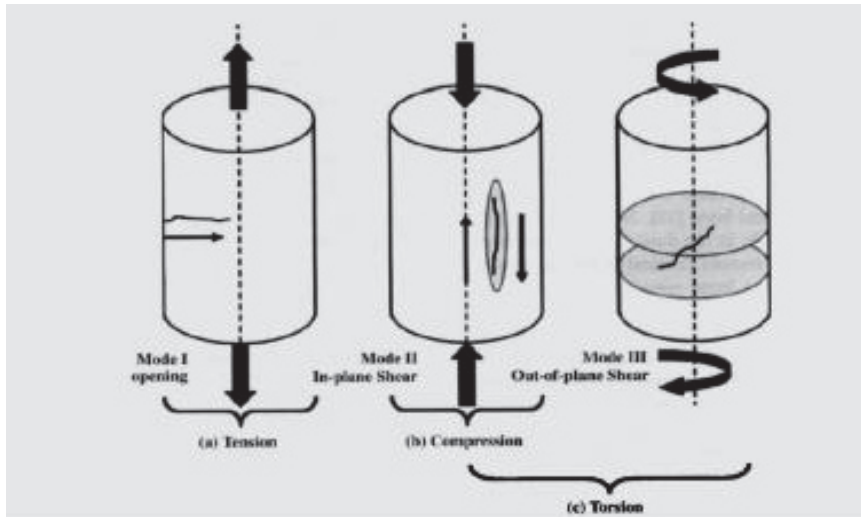


Fig. 5. Schematic representation of microcrack development in specimens subjected to Zero-Tension (Mode I) (a), Zero-Compression (Mode II) (b) and Zero-Torsion (Modes II and III) (c) loading [26]

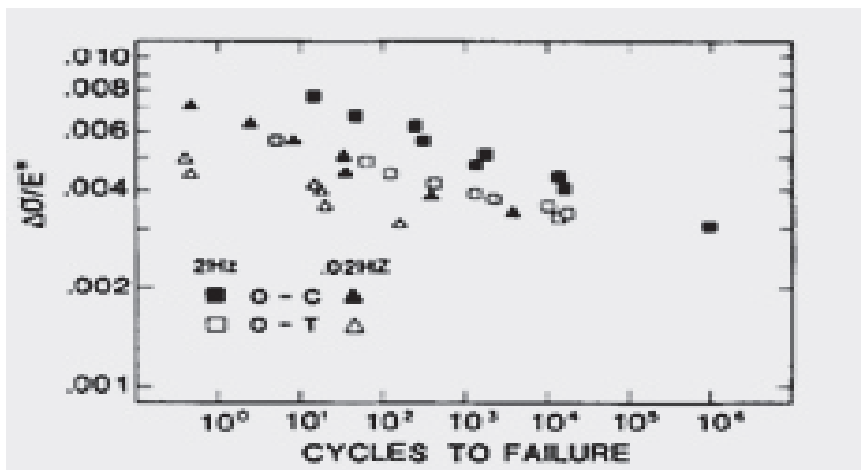


Fig. 6. Tensile (O-T) and compressive (O-C) cyclic loading data plotted as normalized stress versus cycles to failure [20]

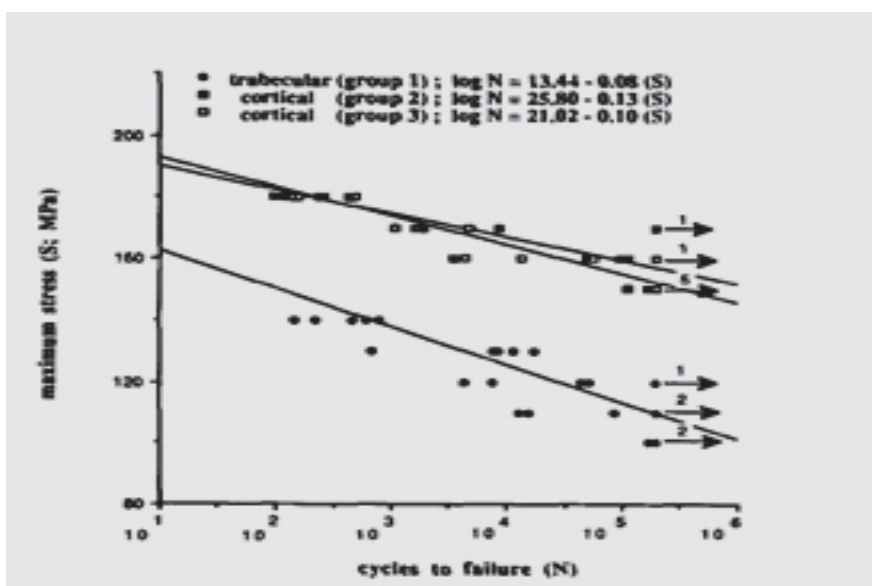


Fig. 7. Median S-N curves for each specimen group. The numbers on arrows indicate the number of run-out specimens for given stress levels [24]

Analysis of permanent strain during tensile fatigue of cortical bone (Fig. 8) shows that ratcheting occurs in cortical bone due to the

cyclic softening of bone. Hence, ratcheting is considered as an irreversible deformation process dependent on the number of cycles.

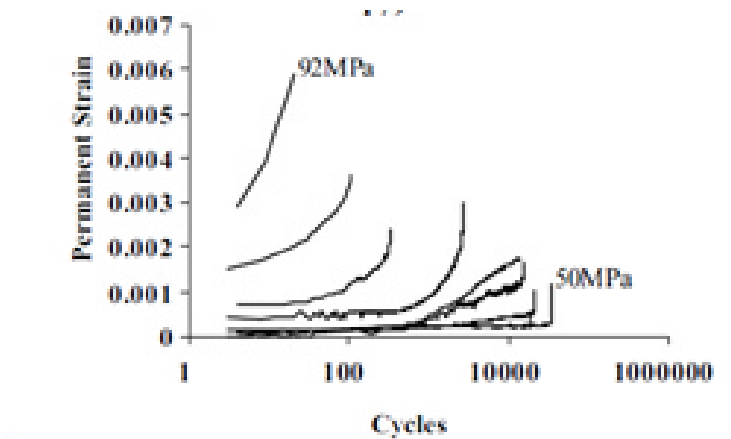


Fig. 8. Ratcheting strain in cortical bone as a function of the number of cycles for different levels of maximum stress [27]

Also, ratcheting was observed experimentally in trabecular bone for specimens subjected to Zero-Compression loading [28-30] and for samples subjected to a combination of torsion and compression fatigue [31]. Systematic studies of ratcheting during tensile, compressive, and shear fatigue of human cortical bone were conducted in [32].

**Cell population dynamics model.** Long term biomechanical adaptation is particularly significant to implant integration and stability in the postoperative state [33]. Wolff's law postulates [14] that bone can be remodeled based on the forces applied during its normal function, modifying its internal and external architecture and changing its shape and density. The remodeling phase of healing can continue for months or even years [34]. Biological cells continuously interact with and remodel the tissue in their immediate environment to establish a well-defined microstructural arrangement in healthy tissue. Local remodeling by cells becomes the crucial connecting point between the biological and mechanical fields [6, 34].

Various mathematical models of bone remodeling have been proposed in the literature [35]. In the present paper, the cell population dynamics model has been considered.

At the cellular scale, bone is composed of (i) bone matrix, infiltrated with minerals and with the osteocyte network; and (ii) vascular pores, containing soft tissues and cells [36]. Changes

in bone microstructure occur by dissolution of old bone matrix by bone-resorbing cells (osteoclasts) and deposition of new bone matrix by bone-forming cells (osteoblasts). The bone remodeling process is governed by the interactions between osteoblasts and osteoclasts through the expression of several autocrine and paracrine factors that control bone cell populations and their relative rate of differentiation and proliferation [37].

The variation in bone density  $\rho$  at the remodeling site is expressed in terms of percentage of the initial mass depending on the number of osteoclasts and osteoblasts [37]:

$$\frac{d\rho}{dt} = k_2 X_B - k_1 X_C$$

Here  $k_1$  and  $k_2$  are the normalized activities,  $X_C$  and  $X_B$  are, respectively, the numbers of actively resorbing osteoclasts and forming osteoblasts at a remodeling site defined by Komarova et al. [38]:

$$\begin{cases} X_C = x_C - \bar{x}_C & \text{if } x_C > \bar{x}_C \\ X_C = 0 & \text{if } x_C \leq \bar{x}_C \end{cases}$$

and

$$\begin{cases} X_B = x_B - \bar{x}_B & \text{if } x_B > \bar{x}_B \\ X_B = 0 & \text{if } x_B \leq \bar{x}_B \end{cases}$$

where  $\bar{x}_c$  and  $\bar{x}_B$  are, respectively, the number of osteoclasts and osteoblasts at steady state. The system of differential equations describing the osteoclast and osteoblast rates and interactions using parameters, which characterize the autocrine and paracrine factors, can be expressed by [37]:

$$\begin{cases} \frac{dx_B}{dt} = \alpha_2 x_C^{g_{12}} x_B^{g_{22}} - \beta_2 x_B \\ \frac{dx_C}{dt} = \alpha_1 x_C^{g_{11}} x_B^{g_{21}} - \beta_1 x_C \end{cases}$$

where  $\alpha_1$  is the osteoclast production rate,  $\beta_1$  is osteoclast removal rate,  $\alpha_2$  is the osteoblast production rate,  $\beta_2$  is the osteoclast removal rate. Parameter  $g_{11}$  describes the combined effects of all the factors produced by osteoclasts that regulate osteoclast formation (osteoclast autocrine regulation). Parameter  $g_{22}$  describes the combined effects of all the factors produced by osteoblasts to regulate osteoblast formation (osteoblast autocrine regulation). Parameter  $g_{12}$  describes the combined effects of all the factors produced by osteoclasts that regulate osteoblast formation, such as TGF $\beta$  (osteoclast-derived paracrine regulation). Parameter  $g_{21}$  describes the combined effects of all the factors produced by osteoblasts that regulate osteoclast formation, such as OPG and RANKL (osteoblast-derived paracrine regulation). In this proposal, special attention is paid to the particular case, where a bone cell grows normally and only influences its neighbor's activity, but does not produce autocrine factors. Therefore, we can write [37].

$$\begin{cases} g_{11} = g_{22} = 0 \\ g_{12} = A_1 + B_1 e^{-\gamma_1 S(x, t)} \\ g_{21} = A_2 + B_2 e^{-\gamma_2 S(x, t)} \end{cases}$$

where  $A_1$ ,  $B_1$ ,  $A_2$ ,  $B_2$ ,  $\gamma_1$ , and  $\gamma_2$  are model parameters that regulate the production of paracrine factors,  $S(x, t)$  denotes the mechanical stimulus function. The mechanical stimulus used here is expressed in terms of strain energy density.

The bone adaptation approach given above allows for the computation of changes in density of femur after advanced core decompression at a discrete site of bone remodeling at a macroscopic scale. In order to simulate the remodeling process from a mechanobiological point of view, this approach needs to be implemented, for example, into an

ANSYS code (considering bone density instead of temperature in the finite element model in Fig. 9).

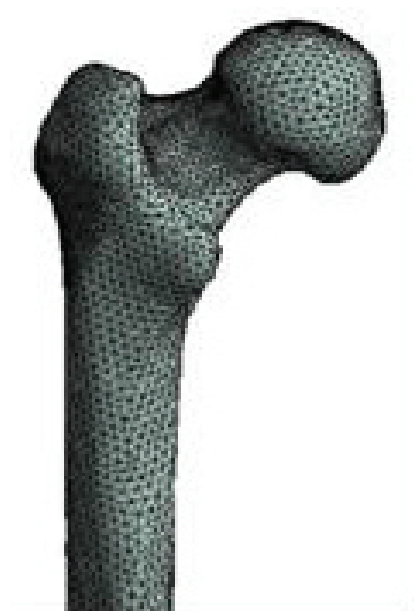


Fig. 9. Finite element model of femur generated by ANSYS [4]

**Structural mechanics model.** The cell population dynamics model needs to be coupled to the structural mechanics model. Total strains in femur are assumed to be composed of nonlinear elastic part, part due to creep and ratcheting part accumulated during cycling loading.

The creep strain rates are related to the stresses under multiaxial loading as follows [39]:

$$\frac{d\varepsilon_{kl}^c}{dt} = \frac{\sigma_e^n}{(1-\phi)^m} \left( \frac{3}{2} \frac{A s_{kl}}{\sigma_i} + C \delta_{kl} \right) \quad (1),$$

where  $\sigma_e = A \sigma_i + C \sigma_{kl} \delta_{kl}$ ,  $\sigma_i = \sqrt{\frac{3}{2} s_{kl} s_{kl}}$ ,  $s_{kl}$  is the stress deviator,  $\sigma_{kl}$  is the stress tensor,  $t$  is time and  $A$ ,  $C$ ,  $n$ ,  $m$  are material parameters. A continuum damage parameter by Kachanov-Rabotnov  $\phi$  has been introduced into the creep law given by Eq. (1) with the formulation of the following creep damage growth equation

$$\frac{d\phi}{dt} = \frac{\Sigma_e^k}{(1-\phi)^l} \quad (2),$$

where  $\Sigma_e = A_0 \sigma_i + C_0 \sigma_{kl} \delta_{kl}$ ,  $A_0$ ,  $C_0$ ,  $k$  and  $l$  are material parameters. Equations (1) and (2) reflect the tension/compression asymmetry of creep and creep damage in femur.

Also, description of ratcheting and fatigue damage in femur is considered. The components of the ratcheting strain tensor can be defined as follows [39]:

$$\dot{\varepsilon}_{kl}^r = \frac{\tau_e^p N^q}{(1-\varphi)^f} \left( \frac{3}{2} \frac{a\kappa_{kl}}{\tau_i} + c\delta_{kl} \right) \quad (3),$$

where  $N$  is a number of cycles,  $\tau_e = a\tau_i + c\tau_{kl}\delta_{kl}$ ,  $\tau_i = \sqrt{\frac{3}{2}\kappa_{kl}\kappa_{kl}}$ ,  $\kappa_{kl}$  is the stress amplitude deviator during cycling,  $\tau_{kl}$  is the tensor of the mean stresses during cycling, dot above the symbol denotes the derivative with respect to the number of cycles, and  $a$ ,  $c$ ,  $p$ ,  $q$  and  $f$  are material parameters. Also, description of ratcheting and fatigue damage in femur is considered. The components of the ratcheting strain tensor can be defined as follows [39]:

$$\dot{\varepsilon}_{kl}^r = \frac{\tau_e^p N^q}{(1-\varphi)^f} \left( \frac{3}{2} \frac{a\kappa_{kl}}{\tau_i} + c\delta_{kl} \right) \quad (3)$$

where  $\rho_e = d\tau_i + e\tau_{kl}\delta_{kl}$ ,  $d$ ,  $e$ ,  $x$ ,  $b$  and  $v$  are material parameters. Equations (3) and (4) reflect the tension/compression asymmetry of ratcheting and fatigue damage in femur.

Note that material parameters in Eqs. (1)-(4) are functions of bone density and bone mineralization, and can be identified from the basic experiments under tension and compression [40].

Diffusion model to describe osteogenesis within a porous Ca PO<sub>4</sub> scaffold needs to be considered. In this regard, the concentration of mesenchymal stem cells can be found using diffusion model developed in [41].

**REFERENCES**

1. Madeo A., George D., Rémond Y. (2013). Second-gradient models accounting for some effects of microstructure on remodelling of bones reconstructed with bioresorbable materials. *Computer methods in biomechanics and biomedical engineering*, 16, 260–261.
2. Ficat R. P., Arlet J. (1980). Necrosis of the femoral head. In: *Ischemia and Necrosis of Bone*. Baltimore: Williams & Wilkins, 53–74.
3. Landgraeber S., Theysohn J. M., Classen T., Jäger M., Warwas S., Hohn H. P., Kowalczyk W. (2013). Advanced core decompression, a new treatment option of avascular necrosis of the femoral head—a first follow-up. *Journal of tissue engineering and regenerative medicine*, 7(11), 893–900.
4. Tran T. N., Kowalczyk W., Hohn H. P., Jäger M., Landgraeber S. (2016). Effect of the stiffness of bone substitutes on the biomechanical behaviour of femur for core decompression. *Medical engineering & physics*, 38(9), 911–916.
5. Madeo A., George D., Lekszycki T., Nierenberger M., Rémond Y. (2012). A second gradient continuum model accounting for some effects of micro-structure on reconstructed bone remodelling. *Comptes Rendus Mécanique*, 340(8), 575–589.

**CONCLUSION**

Analysis of bone density, stress and damage distributions over time in femur after advanced core decompression as well as lifetime prediction studies in this review are related to the consideration of the physically nonlinear initial/three-dimensional boundary value multiphysics problem. Therefore, commercial software package ANSYS needs to be used for structural analysis, computational modeling and simulation, when the integrated constitutive framework discussed in this paper will be implemented into its codes.

The lifetime predictions obtained in this research need to be compared against clinical and experimental data available for femur after core decompression in combination with bone substitutes.

The outcome will be how damage growth in femur after advanced core decompression subjected to mechanical cyclic loading under creep and fatigue conditions may be controlled in order to optimize design and processing of bone graft substitutes, and extend lifetime of bone substitutes.

**PROSPECTS FOR FUTURE STUDIES**

The new knowledge obtained in this research needs to be transferred to research communities related to advanced core decompression. Also, the young professionals training needs to be provided at the Arts et Métiers ParisTech, France, and at the V. N. Karazin Kharkiv National University, Ukraine, on how to use the computer-based structural modeling tool developed in this research.

6. Scala I., Spingarn C., Rémond Y., Madeo A., George D. (2016). Mechanically-driven bone remodeling simulation: Application to LIPUS treated rat calvarial defects. *Mathematics and Mechanics of Solids*, 1081286516651473.
7. Burr D. B. (2011). Why bones bend but don't break. *J Musculoskelet Neuronal Interact*, 11(4), 270-285.
8. Mirzaali M. J., Bürki A., Schwiedrzik J., Zysset P. K., Wolfram U. (2015). Continuum damage interactions between tension and compression in osteonal bone. *Journal of the mechanical behavior of biomedical materials*, 49, 355–369.
9. Reilly, G. C., Currey, J. D. (1999). The development of microcracking and failure in bone depends on the loading mode to which it is adapted. *Journal of Experimental Biology*, 202(5), 543–552.
10. Wolfram, U., Schwiedrzik, J. (2016). Post-yield and failure properties of cortical bone. *BoneKEY reports*, 5. doi:10.1038/bonekey.2016.60
11. Zysset P. K., Schwiedrzik J., Wolfram U. (2016). A statistical damage model for bone tissue based on distinct compressive and tensile cracks. *Journal of biomechanics*, 49(15), 3616–3625.
12. Seref-Ferlengez Z., Kennedy O. D., Schaffler M. B. (2015). Bone microdamage, remodeling and bone fragility: how much damage is too much damage? *BoneKEY reports*, 4. doi:10.1038/bonekey.2015.11
13. Chapurlat R. D., Delmas P. D. (2009). Bone microdamage: a clinical perspective. *Osteoporosis international*, 20(8), 1299–1308.
14. Martin R. B., Burr D. B., Sharkey N. A., Fyhrie D. P. (2015). *Skeletal Tissue Mechanics*. New York: Springer, Second Edition.
15. Bowman S. M., Keaveny T. M., Gibson L. J., Hayes W. C., McMahon T. A. (1994). Compressive creep behavior of bovine trabecular bone. *Journal of biomechanics*, 27(3), 301307–305310.
16. Fondrk M., Bahniuk E., Davy D. T., Michaels C. (1988). Some viscoplastic characteristics of bovine and human cortical bone. *Journal of biomechanics*, 21(8), 623–630.
17. Pollintine P., Luo J., Offa-Jones B., Dolan P., Adams M. A. (2009). Bone creep can cause progressive vertebral deformity. *Bone*, 45(3), 466-472.
18. Deymier-Black A. C., Yuan F., Singhal A., Almer J. D., Brinson L. C., Dunand D. C. (2012). Evolution of load transfer between hydroxyapatite and collagen during creep deformation of bone. *Acta biomaterialia*, 8(1), 253–261.
19. Novitskaya E., Zin C., Chang N., Cory E., Chen P., D'Lima D., Sah R. L., McKittrick J. (2014). Creep of trabecular bone from the human proximal tibia. *Materials Science and Engineering: C*, 40, 219–227.
20. Caler W. E., Carter D. R. (1989). Bone creep-fatigue damage accumulation. *Journal of Biomechanics*, 22(6–7), 625–635.
21. Nilsson, M. K. (2003). *Injectable calcium sulphate and calcium phosphate bone substitutes*. PhD Theses, Lund University.
22. Mostakhdemin M., Amiri I. S., Syahrom A. (2015). *Multi-axial Fatigue of Trabecular Bone with Respect to Normal Walking*. Springer: Singapore.
23. Carter D. R., Caler W. E., Spengler D. M., Frankel V. H. (1981). Uniaxial fatigue of human cortical bone. The influence of tissue physical characteristics. *Journal of Biomechanics*, 14(7), 461–470.
24. Choi K., Goldstein S. A. (1992). A comparison of the fatigue behavior of human trabecular and cortical bone tissue. *Journal of biomechanics*, 25(12), 1371–1381.
25. O'Brien F. J., Taylor D., Lee T. C. (2003). Microcrack accumulation at different intervals during fatigue testing of compact bone. *Journal of Biomechanics*, 36(7), 973–980.
26. George W. T., Vashishth D. (2005). Damage mechanisms and failure modes of cortical bone under components of physiological loading. *Journal of Orthopaedic Research*, 23(5), 1047–1053.
27. Cotton J. R., Zioupos P., Winwood K., & Taylor M. (2003). Analysis of creep strain during tensile fatigue of cortical bone. *Journal of biomechanics*, 36(7), 943–949.
28. Moore T. L. A., O'Brien F. J., Gibson L. J. (2004). Creep does not contribute to fatigue in bovine trabecular bone. *Transaction of ASME. Journal of Biomechanical Engineering*, 126, 321-329.
29. Dendorfer S., Maier H. J., Hammer J. (2009). Fatigue damage in cancellous bone: an experimental approach from continuum to micro scale. *Journal of the mechanical behavior of biomedical materials*, 2(1), 113–119.
30. Haddock S. M., Yeh O. C., Mummaneni P. V., Rosenberg W. S., Keaveny T. M. (2004). Similarity in the fatigue behavior of trabecular bone across site and species. *Journal of biomechanics*, 37(2), 181–187.
31. Fatihhi S. J., Rabiatal A. A. R., Harun M. N., Kadir M. R. A., Kamarul T., Syahrom A. (2016). Effect of torsional loading on compressive fatigue behaviour of trabecular bone. *Journal of the mechanical behavior of biomedical materials*, 54, 21–32.
32. Winwood K., Zioupos P., Currey J. D., Cotton J. R., Taylor, M. (2006). Strain patterns during tensile, compressive, and shear fatigue of human cortical bone and implications for bone biomechanics. *Journal of Biomedical Materials Research Part A*, 79(2), 289–297.

33. Lerebours C., Buenzli P. R. (2016). Towards a cell-based mechanostat theory of bone: the need to account for osteocyte desensitisation and osteocyte replacement. *Journal of Biomechanics*, 49(13), 2600–2606.
34. Buganza Tepole A., Kuhl E. (2016). Computational modeling of chemo-bio-mechanical coupling: a systems-biology approach toward wound healing. *Computer methods in biomechanics and biomedical engineering*, 19(1), 13–30.
35. Lerebours C., Buenzli P. R., Scheiner S., Pivonka P. (2016). A multiscale mechanobiological model of bone remodelling predicts site-specific bone loss in the femur during osteoporosis and mechanical disuse. *Biomechanics and modeling in mechanobiology*, 15(1), 43–67.
36. Buenzli P. R. (2016). Governing equations of tissue modelling and remodelling: A unified generalised description of surface and bulk balance. *Plos one*, 11(4), e0152582.
37. Hambli R. (2014). Connecting mechanics and bone cell activities in the bone remodeling process: an integrated finite element modeling. *Frontiers in bioengineering and biotechnology*, 2(6), 1–12.37.
38. Komarova S. V., Smith R. J., Dixon S. J., Sims S. M., Wahl L. M. (2003). Mathematical model predicts a critical role for osteoclast autocrine regulation in the control of bone modelling. *Bone* 33, 206–215.
39. Altenbach H., Altenbach J., Zolochovsky A. (1995). *Erweiterte Deformationsmodelle und Versagenskriterien der Werkstoffmechanik*. Stuttgart: Deutscher Verlag für Grundstoffindustrie, 172S.
40. Zolochovsky A., Martynenko A., Kühhorn A. (2012). Structural benchmark creep and creep damage testing for finite element analysis with material tension–compression asymmetry and symmetry. *Computers and Structures* 100–101, 27–38.
41. Schmitt M., Allena R., Schouman T., Frasca S., Collombet J. M., Holy X., Rouch P. (2016). Diffusion model to describe osteogenesis within a porous titanium scaffold. *Computer methods in biomechanics and biomedical engineering*, 19(2), 171–179.